



## INVESTIGATION OF THE SEISMIC RESPONSE OF SLENDER PLANAR CONCRETE WALLS

Anna Birely<sup>1</sup>, Laura N. Lowes<sup>2</sup>, Dawn E. Lehman<sup>2</sup>, Ken Marley<sup>3</sup>, Chris Hart<sup>3</sup>, and Dan Kuchma<sup>4</sup>

### ABSTRACT

Structural walls are one of the most commonly used lateral-load resisting systems, and many previous studies have addressed the seismic performance, analysis and design of these systems. However, few previous tests have focused on the performance of structural wall systems and few have simulated the reinforcement patterns and loading distributions found in modern structures. As such, limited data have been available for validation of the models used in performance-based design of these systems. To overcome deficiencies in previous tests, large-scale reinforced concrete walls are being tested using the advanced equipment, control algorithms and instrumentation available at the NEES facility at the University of Illinois. Test specimens include planar, coupled, c-shaped and core wall sub-assemblages. To simulate the demand originating from the upper stories of a multi-story structure, specialized load-and-boundary-condition boxes (LBCBs) are used. Testing of the first series of specimens, four planar walls, was completed in 2008. Data from these tests show the influence of the shear-force distribution and longitudinal reinforcement configuration on wall behavior, drift capacity, the progression of damage, and the contribution to total deformation of flexural, shear, anchorage and other response mechanisms.

### Introduction

Reinforced concrete structural walls are used commonly as the primary lateral-load resisting system for new and retrofit construction. However, despite the heavy reliance on wall systems by practicing engineers, recent efforts to develop performance-based earthquake engineering (PBEE) methods have only just begun to address structural walls. Today engineers have few resources to consult regarding the simulation of wall response using practical linear and nonlinear numerical models or the prediction of wall damage (e.g., concrete crack width and concrete spalling) as a function of engineering demands (e.g., inter-story drift).

A number of issues make the development of performance-based seismic design tools a difficult problem. First, structural walls in modern buildings typically have complex

---

<sup>1</sup>Graduate Research Assistant, Dept. of Civil & Envir. Engineering, University of Washington, Seattle, WA

<sup>2</sup>Associate Professor, Dept. of Civil & Environmental Engineering, University of Washington, Seattle, WA

<sup>3</sup>Graduate Research Assistant, Dept. of Civil Engineering, University of Illinois, Urbana-Champaign, Il.

<sup>4</sup>Associate Professor, Dept. of Civil Engineering, University of Illinois, Urbana-Champaign, Il.

configurations that induce three-dimensional seismic load effects and could be expected to produce significant variation in local damage patterns and ductility demands. Second, few previous experimental investigations provide data that characterize the earthquake response of walls with representative configurations, reinforcement layouts, base conditions and load patterns. Third, few previous experimental investigations provide the high-fidelity response and damage data that are required for development of modern performance-based design tools.

The research presented here represents the first-phase of a multi-year research effort to develop tools to enable performance-based design of structural walls with complex configurations. This multi-year effort includes (i) experimental testing of planar, coupled, and c-shaped wall components as well as a three-dimensional wall system to generate high-resolution response and damage data, (ii) development of model and modeling recommendations to enable simulation of earthquake response of wall structures and prediction of demands, and (iii) development of damage-prediction models for PBEE. This paper presents preliminary results of planar wall tests completed in 2008.

### **Experimental Study**

A priority in the testing program was to develop and evaluate specimens that simulated modern construction. Prior to designing the experimental test specimens, the research team worked with the advisory-panel members to gather information on modern buildings for which walls were the primary lateral load resisting elements. A data set comprising 12 buildings, designed after 1991 by four firms for construction on the West Coast, and including 47 walls with various configurations was assembled. The data collected from the drawings included geometry, reinforcement ratios, and material properties. The data for planar walls (Table 1) were used to identify appropriate ranges for wall geometries characteristics for use in designing the planar wall test specimens. In addition to the geometric, reinforcement and material data, the loading conditions, or effective height of the lateral load, were needed to determine appropriate values of the shear demand-capacity ratios at the base of the wall. The results of previous experimental research (Brown et al. 2006) indicate that failure mode is largely determined by the shear-demand capacity ratio. To determine the possible range of effective heights for mid-rise systems, a series of linear analyses were conducted using one of the buildings from the infrastructure review and effective stiffness reduction factors. The results of this study indicate that effective heights ranging from 0.7 (ASCE-7 (2005) load distribution) to 0.5 are possible.

The objectives of the planar wall test program were to improve understanding of the seismic behavior of planar wall sub-assemblages and to generate high-resolution experimental data characterizing the performance of these sub-assemblages. Based on the reviews of the West Coast building inventory and previous research review, the following gaps in knowledge were identified:

1. The response and performance characteristics of mid-rise walls; most previous tests have focused on 1- to 3-story walls.
2. The effect of the moment gradient and shear demand on the response of mid- to high-rise structural walls.
3. The impact on seismic performance of the longitudinal reinforcement distribution.
4. The influence of a splice at the base of the wall on the seismic performance.

Table 1. Planar wall design characteristics generated from building inventory review

Wall Design Characteristic	Min. Value	Avg. Value	Max. Value	Coeff. of Var.	Prototype Design Value
Thickness	12 in (305 mm)	21.9 in (556 mm)	30 in (762 mm)	0.27	18 in. (457.2 mm)
Length	4.3 ft (1.31 m)	24.3 ft. (7.4 m)	44.5 ft (13.6 m)	0.46	30 ft. (9.1 m)
Boundary-element longitudinal reinf. ratio	1.54%	3.22%	4.70%	0.31	3.5%
Mid-span vert. reinf. ratio	0.21%	0.50%	0.99%	0.58	0.25%
Gross vertical reinf. ratio	0.31%	0.98%	1.81%	0.54	1.4%
Mid-span horiz. reinf. ratio	0.24%	0.46%	1.38%	0.69	0.27%

Table 2 presents the planar wall test matrix, which was developed to address the identified gaps in knowledge. The first specimen, PW1, was intended to represent the bottom three stories of a typical wall designed using the ASCE 7-05 load distribution and following the recommendations of ACI 318-05. It included longitudinal reinforcement that was concentrated in boundary elements at the ends of the wall and spliced at the base of the wall. The ACI 318 Code minimum horizontal reinforcement was provided. Assuming the wall developed nominal flexural strength at its base, the expected shear demand was  $2.8\sqrt{f'_c}$  psi, with  $f'_c$  in psi, corresponding to 66% of the design shear capacity,  $V_n$ , where  $V_n$  was defined per ACI 318-05. Analysis of a representative mid-rise core-wall building suggested that under earthquake loading, inelastic action could result in the effective height of the resultant shear load dropping from that associated with ASCE 7-05 lateral load distribution. This could be expected to result in increased shear demand and impaired performance. Thus, specimens PW2-PW4 were subjected to higher design shear demands of  $4.0\sqrt{f'_c}$  psi, with  $f'_c$  in psi, associated with an effective height for the resultant shear equal to 50% of the building height. PW2 was nominally identical to PW1, with only the base shear demand increased to simulate the reduction in effective height. The third specimen, PW3, was intended to investigate the effect of longitudinal reinforcement layout on performance and included a uniformly distributed longitudinal reinforcement layout of same-sized bars. The fourth specimen, PW4, was intended to investigate the impact of splices on performance and included continuous, un-spliced, longitudinal steel.

Table 2. Planar wall test program (bold values are the design parameters unique to each specimen)

Specimen ID	Effective Height	Design Shear Ratio: $V_{max}/V_n$	Design Shear Stress Demand	Boundary Elements?	Splice?
PW1	<b>0.71</b>	<b>0.66</b>	<b><math>2.8\sqrt{f'_c}</math> [psi]</b> <b><math>0.23\sqrt{f'_c}</math> [MPa]</b>	Yes	Yes
PW2	0.5	0.93	$4.0\sqrt{f'_c}$ [psi] $0.33\sqrt{f'_c}$ [MPa]	Yes	Yes
PW3	0.5	0.93	$4.0\sqrt{f'_c}$ [psi] $0.33\sqrt{f'_c}$ [MPa]	<b>No</b>	Yes
PW4	0.5	0.93	$4.0\sqrt{f'_c}$ [psi] $0.33\sqrt{f'_c}$ [MPa]	No	<b>No</b>

Fig. 1 shows the design of test specimen PW1. On the basis of the data generated from the building inventory review and discussions with consulting engineers, a thickness of 18 in. (457 mm), length of 30 ft. (9.14 m) and story height of 12 ft. (3.7 m) was chosen for the full-scale prototype wall. The laboratory test specimen was intended to representative the bottom three stories of a 10-story building and was tested at 1/3-scale in the laboratory.

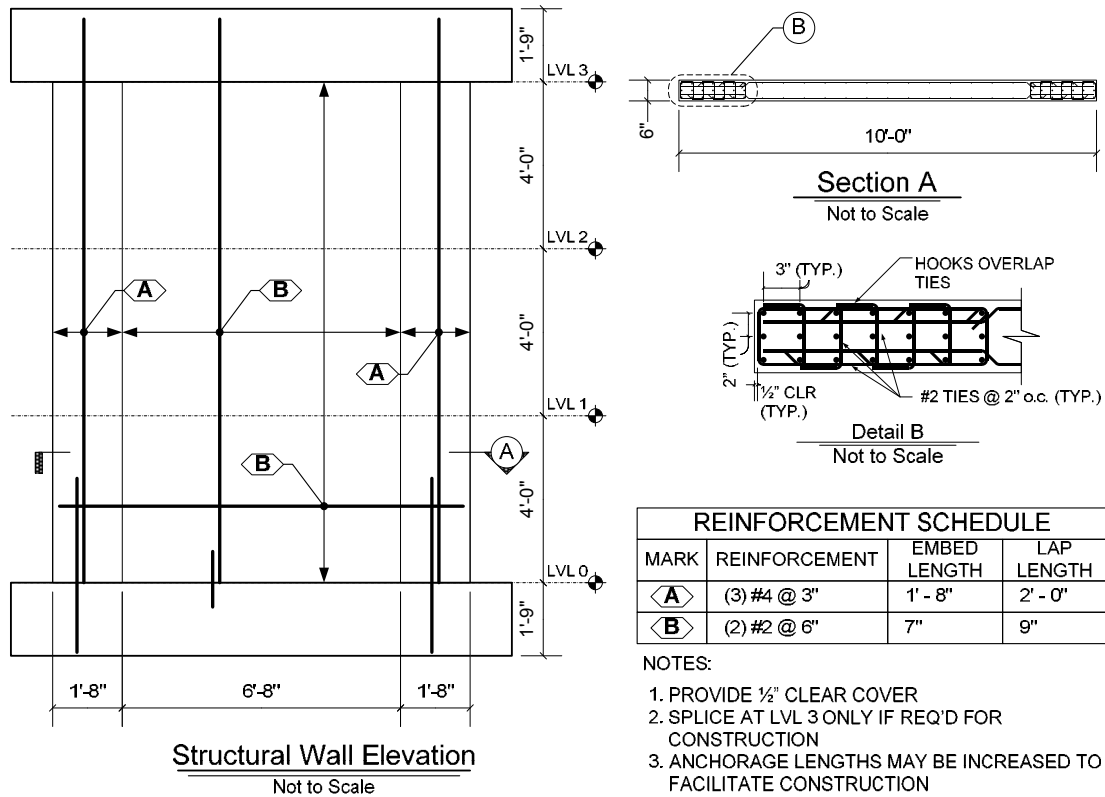


Figure 1. Wall specimen PW1

The NEES “Multi-Axial Full-Scale Sub-Structured Testing and Simulation” (MUST-SIM) facility at the University of Illinois, Urbana-Champaign is being used to conduct the tests. The MUST-SIM facility includes multiple load and boundary condition boxes (LBCBs), each of which comprises six actuators and can be used to apply relatively large loads, in six degrees-of-freedom, under mixed-mode control. For the current study, LBCBs at the top of the specimen applied the shear, moment, and axial load that could be expected to develop in the upper stories of the building under earthquake loading; additional actuators applied shear loads at the top of the 1<sup>st</sup> and 2<sup>nd</sup> stories. Load was applied under displacement controlled; the top of the specimen was subjected to three cycles (two cycles once nominal flexural strength was achieved) each to increasing lateral displacement demands.

### Experimental Results

Preliminary evaluation of the seismic performance of the test specimens was accomplished by considering, for each specimen, the progression of damage during testing, load-displacement history and damage versus drift data.

## Load-Displacement Response

Fig. 2 shows measured base moment versus drift at the top of the specimen for each of the specimens. All specimens had the same nominal flexural design strength; however differences in actual concrete and steel material strengths as well as actual axial loads resulted in significant differences in the nominal flexural strength of the specimens. The data in Fig. 2 show that all specimens achieved the nominal flexural strength of the wall; nominal flexural strength was determined using the procedures outlined in the ACI Code and actual, rather than design, steel yield strength and concrete compressive strength. The data in Fig. 2 show also that drift capacities ranged from 1.0% to 1.5%.

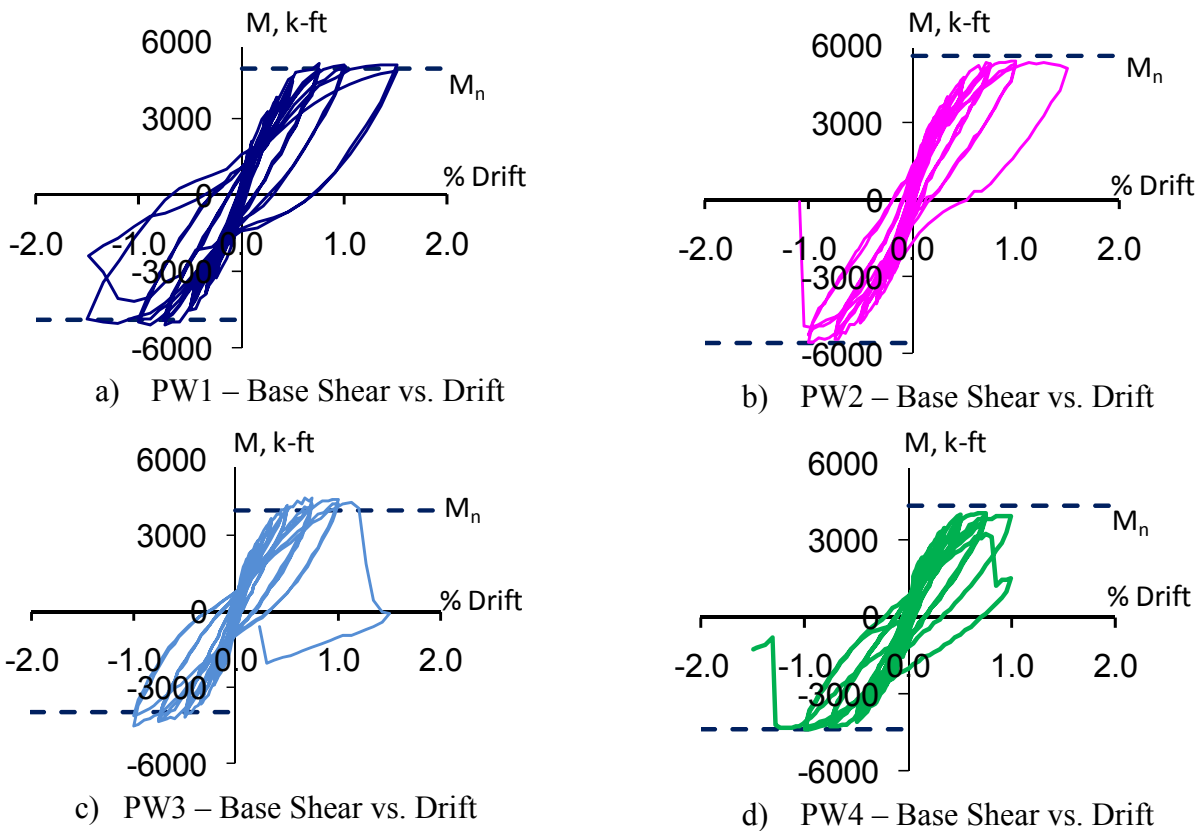


Figure 2. Base moment versus drift at the top of the specimen (1 kip = 4.45 kN)

## Wall Behavior under Cyclic Loading

The following sections describe the progression of damage in the walls under increasing cyclic drift demand. Fig. 3 shows the test specimens at the end of testing.

### *PW1* ( $h_{eff}=0.71h_{10}$ , *BE*, *Splice*)

Specimen PW1 was designed to represent the bottom three stories of a modern planar wall meeting ACI Code (ACI Com. 318 2005) requirements, detailed with heavily reinforced boundary elements, and subjected to shear and moment demands that would result from a standard ASCE-7 load distribution. The progression of damage for PW1 was as follows:

Horizontal cracking of the wall was observed during the 0.1% drift cycle. Diagonal cracking was observed during the 0.15% cycle. Yielding of the longitudinal reinforcement was measured at 0.26% drift. Damage to the concrete was initiated at 0.45% drift, in the form of spalling of the concrete cover at the top of the spliced region. Additional cycling resulted in an increase in the spalled region at the two edges of the walls, with the cover along the spliced region off at the 0.9%-drift level. Larger drift demands and cycling of the specimen resulted in buckling of the longitudinal bars at the top of the spliced region at the 1% drift level. Initiation of loss of lateral capacity occurred during cycling to 1.5% drift due to fracture of the longitudinal reinforcement at the base of the wall. The buckled bars at the top of the spliced region did not fracture; conversely, the bars at the base of the wall (above the footing) did not buckle.



a) PW1 at 1.5% drift    b) PW2 at 1.5% drift    c) PW2 at 1.25% drift    d) PW4 at 1.0% drift  
Figure 3. Wall specimens at the end of testing

#### ***PW2 ( $h_{eff}=0.50h_{10}$ , BE, Splice)***

Specimen PW2 was designed to represent the bottom three stories of a modern planar wall meeting ACI Code requirements, detailed with heavily reinforced boundary elements, and subjected to shear and moment demands that corresponds to an effective height of  $0.5h_{10}$ , where  $h_{10}$  is the total height of the prototype 10-story wall. Damage progression for PW2 was as follows: Diagonal and horizontal cracking initiated at 0.1% drift. Yielding of the reinforcement was measured at 0.2% drift. Concrete spalling initiated at the top of the spliced region at 0.50% drift and at the base of the wall at 0.75% drift. Buckling of the reinforcement occurred at the top of the spliced region at 1% drift. Initiation of core concrete damage in boundary element occurred at 1.5% drift. Lateral capacity was lost during cycling to 1.5% drift due to an apparent compressive failure of the boundary element and web region adjacent to the boundary zone.

#### ***PW3 ( $h_{eff}=0.50h_{10}$ , Uniform, Splice)***

Specimen PW3 was designed to represent the bottom three stories of a modern planar wall meeting ACI Code requirements, detailed with uniformly distributed longitudinal reinforcement, heavy transverse reinforcement in the ACI-defined boundary elements, and subjected to shear and moment demands that corresponds to an effective height of  $0.5h_{10}$ . The specimen was reinforced with No. 4 bars along its length, in contrast to the other specimens, which had No. 2 bars in the interior of the wall. As a result, the height of the spliced bars was at a single plane in Specimen PW3.

Progression of damage for PW3 began with diagonal and horizontal cracking initiated at 0.06% drift. Yielding of longitudinal reinforcement was measured at 0.23% drift. Concrete spalling occurred at the top of the splice region at 0.35% drift. No spalling occurred at the wall base. At 0.75% drift, buckling of the reinforcement occurred at the top of the spliced region and damage to the wall web was initiated. Lateral capacity was lost during the cycle to 1.25% drift due to an apparent compressive failure of the entire web region adjacent to the boundary zone.

#### ***PW4 ( $h_{eff}=0.50h_{10}$ , BE, No Splice)***

Specimen PW4 had a design similar to that of PW1 and PW2 with heavily reinforced boundary elements; however, for PW4 longitudinal reinforcement was not spliced at the base of the wall, as was the case for the previous specimens. Shear and moment demands for the wall were identical to PW2 and PW3, corresponding to an effective height of  $0.5h_{10}$ .

Damage progression for PW4 was as follows: horizontal cracking was observed during at 0.06% drift and diagonal cracking was observed at 0.07% drift. Longitudinal reinforcement yielded at 0.21% drift. Concrete spalling was first observed at 0.35% drift. The 0.75% drift cycles saw buckling of reinforcement and core concrete damage at the base in the East boundary element. This damage became progressively worse until initiation of loss of lateral capacity at 1.0% drift level in an apparent compressive failure. At loss of strength, the West boundary element had only minimal core crushing.

#### **Comparison of Four Walls**

The test results indicate that the effect of the wall study parameters on the seismic performance is significant. Using PW2 as the reference, the impact on performance of the i) load distribution (PW1 in comparison to PW2), ii) distribution of the longitudinal reinforcement (PW2 in comparison to PW3), and iii) splice of wall longitudinal reinforcement above the foundation (PW2 in comparison to PW4) can be assessed.

In all cases, initial damage to the walls included horizontal and diagonal cracking followed by yielding. Damage to the cover concrete always initiated at the top of the spliced region for the first three specimens, whereas cover concrete damage occurred at the base of the wall in the continually reinforced PW4. The next damage state and progression of damage depended on the moment-to-shear (or effective height) of the wall and the distribution of the longitudinal reinforcement, as discussed below.

Specimen PW1 was tested to determine the behavior of a modern wall subjected to the code-specified load distribution. This wall responded in a ductile mode, with loss of lateral capacity resulting from fracture of the longitudinal reinforcement at the base of the wall. Specimen PW2, which was nominally identical to PW1, was subjected to a lower base moment-to-shear ratio, which could occur due to the dynamic response of the system. The resulting response changed from one of flexure to mixed flexure-shear, with concrete damage concentrated at the top of the splice region and spread into the interior of the wall. This change resulted in a reduction in the lateral drift capacity and a sudden loss in lateral strength.

Specimens PW2 and PW3 were subjected to the same moment-to-shear ratios, but had different longitudinal reinforcement distributions. In comparison with PW2, the peak shear strength of PW3 was lower, damage initiated at lower drifts and drift capacity were reduced. Where significant damage in Specimen PW2 initiated at 1.5% drift, for PW3, significant damage in the interior of wall initiated at 0.75% drift and loss of lateral capacity occurred at 1.25% drift. In addition, the damage pattern was altered. Specimen PW2 sustained damage primarily in the boundary element and the adjacent interior portion of the wall. In contrast, Specimen PW3 sustained damage along the entire plane of the wall at the top of the spliced region.

Specimens PW2 and PW4 were subjected to the same moment-shear ratios and had identical longitudinal reinforcement distributions; however, while longitudinal reinforcement was spliced in PW2, it was continuous in PW4. Similar to PW2, damage for PW4 was concentrated in the boundary elements and adjacent portion of the web. While for PW2, damage concentrated at the top of the splice, for PW4 damage occurred lower down at the base of the wall. The order of damage progression in PW4 was the same as PW2, but key damage states were reached earlier in PW4 than in PW2, with base concrete spalling at 0.5% drift (0.75% PW2), bar buckling at 0.75% (1.0% PW2), and core concrete damage occurring at 0.75% (1.5% PW2). Additionally, the lateral drift capacity of PW4 (1.0%) was lower than for PW2 (1.5%), as was the peak shear capacity.

### **Performance Comparison with Previous Tests**

Most past tests of planar concrete walls have employed a single point load at the top of the specimen, resulting in low shear stress demands for slender walls. Because test specimens were not subjected to representative load distributions, the drift defined at the top of the specimen corresponded, approximately, to the roof drift of the walled building. To compare the performance of Specimens PW1-PW4 with past test specimens and assess the impact of load distribution and shear demand on response, a numerical model of the top seven stories of the 10-story prototype wall was used. The computed 10<sup>th</sup>-story (i.e. roof) drift is equal to the 3<sup>rd</sup>-story drift plus some additional drift due to the deformation of the upper stories. In creating the model, it was assumed that significant inelastic action occurred only in the first three stories of the building, which were tested in the laboratory, and that the remaining seven stories of the building remained essentially elastic. Then, for each specimen at each peak in the displacement history, effective elastic flexural and shear cross section stiffnesses were computed using a Timoshenko beam model of the wall. Flexural stiffness values were determined using the applied loads and measured rotations at the base of the wall and the top of the test specimen. Shear stiffness values were determined using the applied load, 3<sup>rd</sup>-story displacement, and calculated flexural stiffness values. For yield cycles, the effective flexural secant stiffness of the wall cross section ranged from  $0.3E_cI_g$  to  $0.5E_cI_g$  and the effective shear stiffness was approximately  $0.1GA$  for all walls. Using these two sets of values to model the top seven stories of the building, the assumption of a Timoshenko beam model, the measured drift and rotation at the top of the specimen, the applied load, and the assumed load distribution for the building, the drift at the top of the building was computed. The computed roof drift for the 10-story building was nominally identical using cross section flexural stiffnesses of  $0.3E_cI_g$  and  $0.5E_cI_g$ .



Fig. 4 shows damage versus drift for the current test specimens as well as for previously tested walls (Brown 2008). Damage is characterized by six damage states (DS) that describe the extent of concrete cracking, spalling, crushing, and loss of lateral strength:

- DS 0 - First recorded horizontal crack.
- DS 1 - First recorded diagonal crack.
- DS 2 - Recorded yield of extreme reinforcement.
- DS 3 - Reported spalling of concrete cover.
- DS 4 - Reported crushing of the web concrete.
- DS 5 - Extreme damage including a) buckling of the reinforcement or b) damage resulting in the reduction of lateral strength by 20%.

These DS were defined primarily on the basis of the repair techniques. However, in the past, damage data were not rigorously collected during laboratory tests; thus, these broad damage categories also reflect the limited nature of the damage data available in the literature.

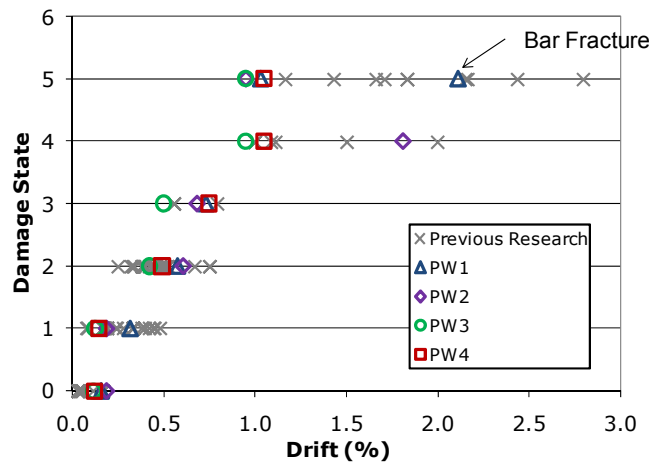


Figure 4. Damage-drift data for current and prior wall tests. Computed roof drift data are presented for PW1-PW4.

The data in Fig. 4 show that the current specimens sustained more moderate levels of damage (e.g., cracking and yielding) at similar drift levels as the prior test specimens. However, more significant damage states, such as web crushing and damage resulting in strength loss, typically occurred at lower drift levels. It should be noted that Specimen PW1 sustained DS 5, bar buckling at a drift of 1.0% and then DS 5, bar fracture at a drift in excess of 2.0%. The data in Fig. 4 suggest that performance-prediction tools developed using previous test data may not accurately reflect the true performance of walls.

## Conclusions

A NSF-sponsored research program is underway to develop tools and technologies to enable performance-based design of structural reinforced concrete walls. As part of this project, a series of large-scale planar wall sub-assemblages were tested using the advanced experimental capabilities of the NEES UIUC MUST-SIM Laboratory facility. The walls were constructed using modern wall details and designed to simulate the lower three stories of a ten-story prototype building. The capabilities of the load-and-boundary-condition boxes (LBCBs) permitted the application of moment, shear and axial load to the top of the wall, thereby

permitting the top of the experimental wall to be subjected to the demands resulting from the upper stories of the prototype structure. In addition, changing the moment-to-shear ratio permitted different load distributions to the wall, to better simulate the effect on seismic performance of both dynamic loading and changes in the wall stiffness. Preliminary results and observations of these laboratory tests are as follows:

1. Damage always initiated at the top of the splice, suggesting that the splice impacts seismic performance.
2. Even for a wall with ductile detailing, altering the moment-to-shear (or effective height) of the wall can significantly impact the response mode that causes loss of lateral capacity. In the walls tested, this difference changed the determining response mode from flexure to compression-shear in the boundary zone.
3. A reduction in the effective height had a significant impact on the drift capacity. The lower effective height resulted in a reduction of the cyclic response capacity as well as a more sudden loss of strength.
4. Specimen PW3 was detailed with the same longitudinal bar size uniformly distributed along its length, all of which was spliced at the base. In this wall, damage initiated in the interior and progressed to the sides where as for Specimen PW2 damage initiated at the boundary elements. In addition, damage in the uniformly reinforced wall occurred at a single plane, located at the top of the spliced region. This damage mode resulted in earlier initiation of damage as well as a reduction in the wall drift capacity.

### **Acknowledgements**

The authors would like to acknowledge the contributions of graduate student researchers Peter Brown, Paul Oyen, and Aaron Sterns from the University of Washington and Jun Ji from the University of Illinois. The authors would also like to acknowledge the contributions of Professor Emeritus Neil Hawkins; Ron Klemencic and John Hooper of Magnusson Klemencic Associates, Seattle; Andrew Taylor, of KPFF, Seattle and Joe Maffei, of Rutherford & Chekene, San Francisco in advising the practical aspects of the research program. The research presented herein was funded by the National Science Foundation through the Network for Earthquake Engineering Simulation (NEES) Program, grant CMMI-0402490, and the NEES Research Program, grant CMS-042157.

### **References**

- ACI, 2005. *Building code requirements for structural concrete (ACI 318-05) and commentary (ACI 318R-05)*, American Concrete Institute, Farmington Hills, Michigan.
- ASCE, 2005. *Standard-Minimum Design Loads for Buildings and Other Structures (ASCE 7-05)*, American Society of Civil Engineers, Reston, VA.
- Brown, P., 2008. Probabilistic Earthquake Damage Prediction for Reinforced Concrete Building Components, *M.S. Thesis*, University of Washington, Seattle.